

Leveling of MHD turbulence imbalance in shear flows

Mariami Kavtaradze,^{1,2} George Mamatsashvili,^{3,1,*} George Chagelishvili,^{1,4} and Elene Uchava¹

¹*Abastumani Astrophysical Observatory, Abastumani 0301, Georgia*

²*Department of Physics, Faculty of Exact and Natural Sciences, Tbilisi State University, Tbilisi 0179, Georgia*

³*Helmholtz-Zentrum Dresden-Rossendorf, Bautzner Landstr. 400, D-01328 Dresden, Germany*

⁴*M. Nodia Institute of Geophysics, Tbilisi 0193, Georgia*

(Dated: February 17, 2026)

We investigate magnetohydrodynamic (MHD) turbulence in plane shear flows with a streamwise background magnetic field in the super-Alfvénic regime. We show that the large-scale velocity shear suppresses turbulence imbalance, driving the system toward a balanced state – the energies of counter-propagating Alfvén waves become essentially equal, even at initially perfectly imbalanced Alfvénic turbulence. This balancing is due to the shear-induced linear non-modal dynamics of Alfvén waves, including their transient growth and over-reflection. This linear route to balancing turbulence is new – fundamentally different from nonlinear ones operative in shearless MHD turbulence – and have direct implications for understanding balanced/imbalanced MHD turbulence in the solar wind, which is modeled as a shear flow in a thermodynamically complex plasma.

Turbulence in magnetized plasmas, often described within magnetohydrodynamics (MHD), is widespread in natural and laboratory settings. Its first theoretical model was proposed by Iroshnikov [1] and Kraichnan [2] as an extension of Kolmogorov's [3] theory of isotropic hydrodynamic turbulence, incorporating a magnetic field but still assuming isotropy. Later, Goldreich and Sridhar [4] dropped this limitation and addressed anisotropy of MHD turbulence, which is naturally caused by a mean magnetic field. In the presence of the mean field, Alfvén waves with two different polarizations — pseudo-Alfvén and shear-Alfvén waves — arise in incompressible MHD, each of which consists of counter-propagating components. An important factor in MHD turbulence is the difference between amplitudes of these counter-propagating waves, which determines the balanced/imbalanced nature of the turbulence and which has been extensively studied (e.g., [5–11]). The growing interest in this area is largely motivated by observations of solar wind (e.g. [12–15]). Studying the degree of imbalance in MHD turbulence is essential to understand energy and momentum transfers across scales (e.g., [8, 10, 16, 17]) as well as heating and particle acceleration [18]. These processes are crucial for interpreting astrophysical and heliospheric (e.g., solar wind) plasma observations.

In these settings, magnetized plasma, as a rule, exhibits large-scale inhomogeneous kinematics, or shear flows that act as a significant source of dynamical activity. For example, shear flows in the solar wind have long been recognized as a source of turbulence therein [19–24]. Of course, in astrophysical plasma flows, complex thermodynamic effects act alongside kinematic ones. Nevertheless, shear is the main energy source of turbulence in the flow. So, neglecting thermodynamic factors, we aim to grasp shear-driven processes constituting the core of turbulence dynamics.

Shear flow – a driver of plasma dynamics – is a likely factor determining also the balanced/imbalanced nature of MHD turbulence. Observations of the solar wind indicate that, despite being mostly imbalanced, regions of balanced turbulence also exist that coincide with strong velocity shear regions [20, 21, 25–30]. This has motivated us to investigate the physics of the influence of shear on the degree of imbalance of MHD turbulence in detail.

Previous studies of forced, strong, imbalanced turbulence [9, 31] showed that numerical simulations are sensitive to the forcing method, complicating the description of the inertial range and energy spectra in Fourier space. However, in shear flow turbulence, the inertial range, which is a range of action of nonlinear processes only, is strictly speaking absent, because both shear-induced linear and nonlinear processes operate, in principle, in parallel over a broad range of wavenumbers [32–34]. This naturally calls into question the applicability of the inertial range concept in shear flows. Specifically, shear flows are non-self-adjoint that results in linear transient, or non-modal growth of perturbations (e.g., [35–38] and references therein), which depends on the orientation of their wavevector and hence is anisotropic in Fourier space [34, 39, 40]. However, because of its transient character, the non-modal growth itself is imperfect and requires nonlinear positive feedback to continuously operate and energetically supply turbulence. Such a feedback is ensured by the *nonlinear transverse cascade* – a generic nonlinear process in shear flows that is caused by the shear and hence is topologically distinct (anisotropic) from conventional (inverse/direct) nonlinear cascades [32, 33]. The refined interplay between linear non-modal growth and nonlinear transverse cascade is responsible for the sustenance of turbulence in both hydrodynamic and MHD shear flows [33, 34, 41–43].

In this Letter, we investigate the dynamics of MHD turbulence in plane shear flows, focusing on its balanced/imbalanced nature. It is shown that strong enough shear can reduce the degree of turbulence imbalance for any initial ratio of amplitudes of pseudo- and shear-

* g.mamatsashvili@hzdr.de

Alfvén waves. This balancing of turbulence is largely due to the linear non-modal dynamics of the Alfvén waves, whose linear coupling results in their non-modal growth and over-reflection [44, 45]. Thus, this Letter presents a novel view on the nature of balance/imbalance of MHD turbulence in shear flows based on the non-modal processes of Alfvén waves rather than by their nonlinear interactions as is the case in classical (i.e., shearless and forced) MHD turbulence.

We consider an unbounded isentropic plane flow along the y -axis with a constant shear $S > 0$ of velocity along the x -axis, $\mathbf{U}_0 = -Sx\mathbf{e}_y$, in the Cartesian coordinate system (x, y, z) , where \mathbf{e}_y is the unit vector along the y -axis. The flow is subject to a uniform streamwise magnetic field $\mathbf{B}_0 = B_{0y}\mathbf{e}_y$, $B_{0y} > 0$. Due to its thermodynamical simplicity, this basic model of a magnetized shear flow allows us to focus on and understand shear effects on MHD turbulence. The perturbations of velocity \mathbf{u} and magnetic field \mathbf{b} about this base flow are governed by the equations of incompressible MHD

$$\frac{D\mathbf{u}}{Dt} + (\mathbf{u} \cdot \nabla)\mathbf{u} - Su_x\mathbf{e}_y = -\frac{1}{\rho}\nabla P + (\mathbf{U}_A \cdot \nabla)\mathbf{b} + (\mathbf{b} \cdot \nabla)\mathbf{b} + \nu\Delta\mathbf{u}, \quad (1)$$

$$\frac{D\mathbf{b}}{Dt} = -Sb_x\mathbf{e}_y + (\mathbf{U}_A \cdot \nabla)\mathbf{u} + \nabla \times (\mathbf{u} \times \mathbf{b}) + \eta\Delta\mathbf{b} \quad (2)$$

with the divergence-free conditions $\nabla \cdot \mathbf{u} = \nabla \cdot \mathbf{b} = 0$, where ρ is the constant density, P is the total, a sum of the thermal and magnetic, pressures and $\mathbf{U}_A = \mathbf{B}_0/(4\pi\rho)^{1/2}$ is the Alfvén velocity corresponding to the background field \mathbf{B}_0 . Here $D/Dt \equiv \partial/\partial t - Sx\partial/\partial y$ is the derivative along the base flow. The field perturbation is measured in velocity units, $\mathbf{b}/(4\pi\rho)^{1/2} \rightarrow \mathbf{b}$. Following MHD turbulence approach [4, 9], we rewrite Eqs. (1)–(2) for Elsässer variables, $\mathbf{Z}^\pm = \mathbf{u} \pm \mathbf{b}$:

$$\left(\frac{D}{Dt} \mp \mathbf{U}_A \cdot \nabla \right) \mathbf{Z}^\pm + (\mathbf{Z}^\mp \cdot \nabla) \mathbf{Z}^\pm = -\nabla P + SZ_x^\mp \mathbf{e}_y + \frac{\nu + \eta}{2} \Delta \mathbf{Z}^\pm + \frac{\nu - \eta}{2} \Delta \mathbf{Z}^\mp, \quad \nabla \cdot \mathbf{Z}^\pm = 0. \quad (3)$$

The term $SZ_x^\mp \mathbf{e}_y$ proportional to shear in these equations plays a central role – it is responsible for the linear coupling of counter-propagating Alfvén waves, characterized by \mathbf{Z}^\pm , and for their energy exchange with the base flow. By contrast, in the classical case without shear, these waves are coupled only through the nonlinear term $(\mathbf{Z}^\mp \cdot \nabla) \mathbf{Z}^\pm$. Our main goal is to analyze the influence of the shear-induced linear coupling of Alfvén waves (i.e., their Elsässer variables) on the dynamics of MHD turbulence and, in particular, on its imbalance.

We stress that shearless MHD turbulence considered in most studies is fueled by some external forcing (e.g., [4, 9, 10, 46]), whereas here we study the turbulence with an intrinsic energy source – the base MHD shear flow \mathbf{U}_0 , as is usually the case in natural settings. This

constant shear flow subject to a uniform streamwise field is modally stable, i.e., it has no exponentially growing modes according to the modal analysis [47–49]. However, as noted above, in shear flows, perturbations undergo non-modal growth, which serves (via the term $SZ_x^\mp \mathbf{e}_y$) as the basic energy supplier for turbulence [33, 34].

One of the central characteristics of MHD turbulence is the total cross-helicity $H_c = \int(\mathbf{u} \cdot \mathbf{b})dV = (1/4)\int[(Z^+)^2 - (Z^-)^2]dV$ (the integral is taken over the domain), which measures the degree of turbulence imbalance, that is, the difference between the Elsässer energies $(1/4)\int(Z^+)^2dV$ and $(1/4)\int(Z^-)^2dV$ of counter-propagating Alfvén waves. In the ideal case without shear, H_c is conserved if perturbations obey periodic boundary conditions or vanish at infinity [50], implying the conservation of the imbalance/balance of turbulence. However, in shear flows $S \neq 0$ and it follows from Eqs.(1) and (2) that H_c becomes time-dependent

$$\frac{dH_c}{dt} = S \int (u_x b_y - u_y b_x) dV = \frac{S}{2} \int (Z_x^- Z_y^+ - Z_x^+ Z_y^-) dV$$

that can have consequences for the turbulence imbalance, as shown below.

We decompose the perturbations into spatial Fourier harmonics, $f(\mathbf{r}, t) = \int \tilde{f}(\mathbf{k}, t) \exp(i\mathbf{k} \cdot \mathbf{r}) d^3\mathbf{k}$ to classify their modes, where $f \equiv (\mathbf{u}, \mathbf{b})$ and bar denotes Fourier transforms. There are two types of linear modes in the flow: (i) Alfvén waves, which oscillate with frequencies $\omega = \pm U_A k_y$ (without shear) each for \mathbf{Z}^\pm , where $k_y \neq 0$ is the wavenumber along the y -axis parallel to \mathbf{U}_0 and \mathbf{B}_0 , and (ii) non-oscillatory, uniform in the streamwise y -direction ($k_y = 0$) modes, which have independent magnetic and velocity perturbations. The Alfvén wave mode can be further divided into pseudo-and shear-Alfvén waves according to their polarizations [4, 45], which in Fourier space take the form:

Pseudo-Alfvén wave (PAW) with velocity $\bar{\mathbf{u}}_p = (\bar{u}_x, -k_x \bar{u}_x/k_y, 0)$ and magnetic field $\bar{\mathbf{b}}_p = (\bar{b}_x, -k_x \bar{b}_x/k_y, 0)$ perturbations lying in (x, y) -plane (k_x is the wavenumber along the x -axis) and the corresponding Elsässer fields $\bar{\mathbf{Z}}_p^\pm = (\bar{Z}_x^\pm, -k_x \bar{Z}_x^\pm/k_y, 0)$.

Shear-Alfvén wave (SAW) with velocity $\bar{\mathbf{u}}_s = (0, -k_z \bar{u}_z/k_y, \bar{u}_z)$ and magnetic field $\bar{\mathbf{b}}_s = (0, -k_z \bar{b}_z/k_y, \bar{b}_z)$ perturbations lying in (y, z) -plane perpendicular to the flow and magnetic field (k_z is the wavenumber along the z -axis) and the corresponding Elsässer fields $\bar{\mathbf{Z}}_s^\pm = (0, -k_z \bar{Z}_z^\pm/k_y, \bar{Z}_z^\pm)$.

Note that since PAW have nonzero \bar{Z}_x^\pm , only they can directly exchange energy with the base flow due to shear via the linear term $SZ_x^\mp \mathbf{e}_y$ in Eq. (3). As a result, PAW undergoes linear non-modal growth, including the process of over-reflection of a counter propagating PAW branch [45]. Namely, if, say, only \mathbf{Z}_p^+ is initially imposed in the flow, then evolving with time it undergoes non-modal growth, accompanied by the emergence of \mathbf{Z}_p^- with higher amplitude. As for SAW, it gains energy not from the base flow (since its $Z_x^\pm = 0$) but from PAW via shear-induced linear coupling to the latter [45].

M_A	$\langle\langle E_K \rangle\rangle$	$\langle\langle E_M \rangle\rangle$	$\langle u_x u_y \rangle$	$\langle -b_x b_y \rangle$
∞	1.527	—	0.404	—
10	0.973	0.256	0.170	0.020
5	0.699	0.210	0.123	0.020
3.3	0.630	0.205	0.092	0.018

TABLE I. Simulation parameters: Alfvén Mach number M_A , including the hydrodynamic case $M_A = \infty$, and the volume- and time-averaged (denoted by double brackets) kinetic, E_k , and magnetic, E_m , energy densities as well as the Reynolds, $u_x u_y$, and Maxwell, $-b_x b_y$, stresses in the turbulent state.

Thus, the linear non-modal process (growth) is the main energy supplier for PAW, which in turn exchanges energy with and excites SAW via linear coupling as well as via nonlinearity. That is, PAW is energetically dominant in the presence of shear and hence its shear-induced coupling with SAW necessitates accounting for PAW in sheared MHD turbulence. By contrast, in shearless MHD turbulence driven by external forcing, SAW is generally assumed to play a dominant role, whereas PAW is usually neglected [4, 11, 46, 51].

We solve the main Eqs. (1)-(2) using the pseudo-spectral code SNOOPY [52] in a cubic domain with sizes $(L_x, L_y, L_z) = (2\pi, 2\pi, 2\pi)$ and resolution $(N_x, N_y, N_z) = (256, 256, 256)$. As is customary in simulations of constant shear flows without rigid boundaries, the boundary conditions are periodic in y and z , but shear-periodic in x (e.g., [53–55]).

We non-dimensionalize time by S^{-1} , length by some arbitrary length scale ℓ of the order of the flow system size, velocity by $S\ell$ (magnetic field is measured in velocity units too) and energy densities by $\rho_0 S^2 \ell^2$. The main parameters of the problem are the Reynolds $Re = S\ell^2/\nu$ and magnetic Reynolds $Rm = S\ell^2/\eta$ numbers, which are fixed to $Re = Rm = 1000$, and Alfvén Mach number $M_A = S\ell/U_A = (4\pi\rho)^{1/2} S\ell/B_{0y}$ measuring the strength of the background field. It was shown in [33, 45] that the effect of shear on the dynamics of Alfvén waves is important when their frequency is smaller or comparable to the shear, $\omega_A = U_A k_y \lesssim S$, or in non-dimensional units $k_y/M_A \lesssim 1$. For this condition to hold in our domain at least for the smallest $k_{y,\min} = 2\pi/L_y = 1$, one gets $M_A \gtrsim 1$, that is, the *super-Alfvénic regime*, which we focus on below.

The simulations are initialized by small amplitude random noise perturbations of velocity and magnetic field with equal weights of PAW, SAW and streamwise uniform $k_y = 0$ modes. We considered different M_A , including the hydrodynamic ($\mathbf{b} \equiv 0$ and $M_A = \infty$) case, which are all listed in Table I. The initial perturbations undergo non-modal amplification due to shear and after several shear times their amplitude becomes sufficiently high to reach a nonlinear regime. As a result, the flow eventually settles down into a quasi-steady bursting MHD turbulence, as shown in Fig. 1. Since the base flow is modally stable, this turbulence is sub-

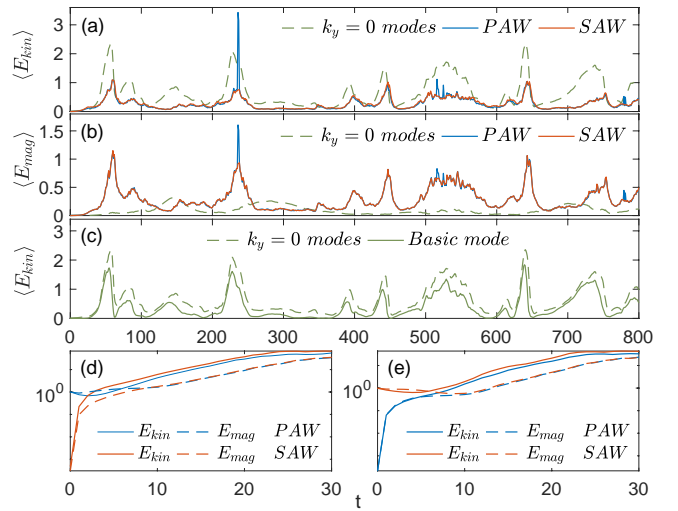


FIG. 1. Evolution of the volume-averaged (a) kinetic $\langle E_k \rangle$ and (b) magnetic $\langle E_m \rangle$ energies of PAW, SAW and $k_y = 0$ modes for the initially imposed PAWs. (c) Kinetic energy of the basic mode together with that of the $k_y = 0$ modes. (d) The same evolution of the wave energies as in (a) and (b), but at early times and normalized by the initial values. (e) The same as in (d) but for initially imposed SAWs.

critical. The time- and volume-averages of the kinetic, $E_k = \mathbf{u}^2/2$, and magnetic, $E_m = \mathbf{b}^2/2$, energy densities as well as the Reynolds, $u_x u_y$, and Maxwell, $-b_x b_y$, stresses are given in Table I. Note that the kinetic energy and Reynolds stress are larger than the magnetic energy and Maxwell stress, respectively, implying that the turbulence is driven mainly by hydrodynamic non-modal processes [34, 56]. Both energies and stresses decrease with decreasing M_A , i.e., with reducing the shear or increasing the field strength, and at a critical $M_{A,c} \approx 3$ the flow transitions from turbulent to laminar.

Having described the general properties of the MHD turbulence in the flow, we focus next on our main goal – analysis of the large-scale velocity shear effects on the balance/imbalance dynamics of this turbulence. We take $M_A = 10$, that is, the strongly super-Alfvénic regime, as is typically observed in the solar wind near the Earth [27, 57]. We consider different, perfectly imbalanced, initial conditions consisting of random perturbations of: (i) only PAWs with rms amplitude $\langle (Z_p^+)^2 \rangle^{1/2} = 0.14$ and $Z_p^- = Z_s^\pm = 0$ and (ii) only SAWs with rms amplitude $\langle (Z_s^+)^2 \rangle^{1/2} = 0.16$ and $Z_s^- = Z_p^\pm = 0$. The $k_y = 0$ modes are initially absent in both cases. Other imbalanced initial conditions with $Z_{p,s}^- \neq 0$ and $Z_{p,s}^+ = 0$ exhibit qualitatively similar evolution and are not shown here.

Figure 1 shows the evolution of the volume-averaged kinetic, $\langle E_k \rangle$, and magnetic, $\langle E_m \rangle$, energies of PAWs and SAWs with $k_y \neq 0$ as well as $k_y = 0$ modes, starting from the perfectly imbalanced states described above. The kinetic and magnetic energies of PAWs and SAWs each are almost equal at all times [Figs. 1(a) and 1(b)], that is, there is equipartition between the PAW and SAW ener-

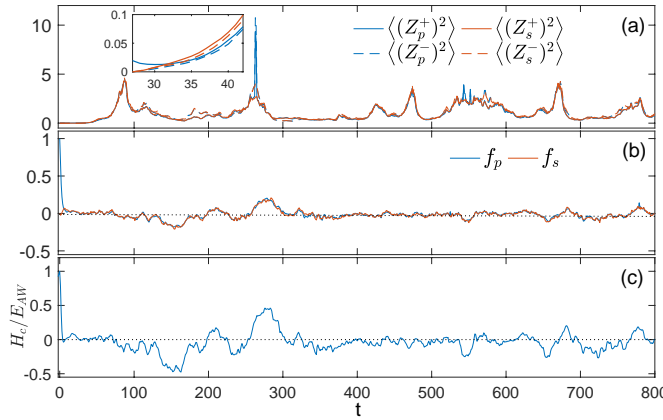


FIG. 2. Evolution of (a) the volume-averaged Elsässer energies $\langle (Z_p^\pm)^2 \rangle$ and $\langle (Z_s^\pm)^2 \rangle$ for PAWs (blue) and SAWs (red), respectively, for the initially imposed only PAWs, (b) the ratios f_p and f_s (see text) and (c) the normalized cross-helicity with small time-average 0.04 in the turbulent state.

gies in contrast to MHD turbulence without shear, where, as noted above, only SAWs play a role. As for the $k_y = 0$ modes, they undergo occasional rapid non-modal growth events, or bursts [Fig. 1(c)], which are in fact associated with the bursts of the dominant $\mathbf{k}_b = (0, 0, 2\pi/L_z)$ mode, referred to as the *basic mode*, as it carries the highest energy among all the $k_y = 0$ modes. During these bursts, the basic mode nonlinearly transfers energy to the Alfvén waves, giving rise to similar bursts in the wave energies with a slight time lag [Fig. 1(a)]. In contrast to the waves, the $k_y = 0$ modes remain essentially hydrodynamic, because their magnetic energy is much smaller than kinetic one and smaller than the magnetic energy of the waves. This bursty dynamics of the basic mode, and so all the $k_y = 0$ modes, is governed by the interplay of the primarily hydrodynamic linear non-modal growth and nonlinear processes [34, 56].

Although the evolution of the PAW and SAW energies is quite similar in the turbulent state, their early-time development for the considered two perfectly imbalanced initial states with only PAWs or SAWs differs due to the essentially different linear dynamics of these waves, as noted above. In the first case, initially imposed PAWs undergo non-modal growth (over-reflection) and also cause SAWs to rapidly grow due to linear coupling [Fig. 1(d)]. However, in the second case, the growth of the imposed SAWs is slower – they initially excite PAW due to nonlinearity, which in turn non-modally grow and reinforce the originally imposed SAWs [Fig. 1(e)].

Figures 2(a) and 2(b) show the evolution of the volume-averaged Elsässer energies of PAWs and SAWs as well as the corresponding ratios $f_p = \langle (Z_p^+)^2 - (Z_p^-)^2 \rangle / D$, $f_s = \langle (Z_s^+)^2 - (Z_s^-)^2 \rangle / D$, where $D = \langle (Z_p^+)^2 + (Z_p^-)^2 + (Z_s^+)^2 + (Z_s^-)^2 \rangle$, which measure the degree of imbalance for each of these wave branches. It is clear that the initially imposed only PAWs with nonzero $Z_p^+ \neq 0$ (i.e., $f_p(0) = 1, f_s(0) = 0$), its coun-

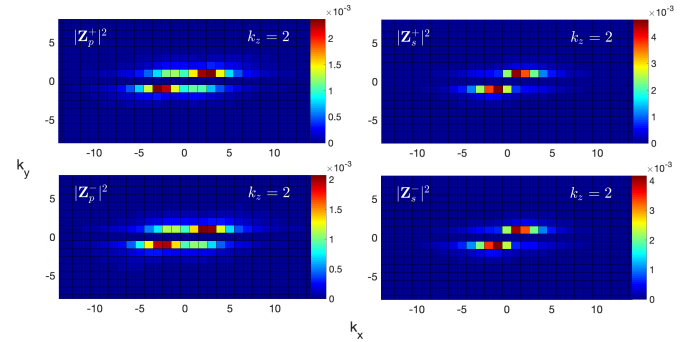


FIG. 3. Spectra of $|\bar{Z}_p^\pm|^2$ (left) and $|\bar{Z}_s^\pm|^2$ (right) in the (k_x, k_y) -plane at $k_z = 2$ in the turbulent state.

terpart Z_p^- generated as a result of non-modal growth (over-reflection) and Z_s^\pm of SAWs excited due to linear coupling with these PAWs all become remarkably close to each other in the turbulent state: $\langle (Z_p^+)^2 \rangle \approx \langle (Z_p^-)^2 \rangle \approx \langle (Z_s^+)^2 \rangle \approx \langle (Z_s^-)^2 \rangle$. Thus, there is equipartition not only between the Elsässer energies of PAWs and SAWs (Fig. 1), but also between Z^+ and Z^- for each of these Alfvén wave branches. Accordingly, f_p rapidly drops from its initial value of 1 and fluctuates near zero in the turbulent state, while f_s remains equal to f_p at all times. This indicates that the turbulence is on average balanced in time despite being imbalanced initially. This is further confirmed by the evolution of the normalized cross-helicity H_c/E_{AW} in Fig. 2(c), where E_{AW} is the total energy of PAWs and SAWs. This efficient exchange among all four Alfvén wave branches – counter-propagating two PAWs (Z_p^\pm) and two SAWs (Z_s^\pm) – which results in the emergence of this balanced state from an initially imbalanced one, is therefore due to shear-induced non-modal mechanism. Indeed, in the classical shearless case, Elsässer fields interact only nonlinearly that does not change their total energies $(1/4) \int (Z_{p,s}^+)^2 dV$ and $(1/4) \int (Z_{p,s}^-)^2 dV$, and hence the degree of imbalance in time [4].

We also examined the spectrum of Alfvén waves, which is one of the key characteristics of MHD turbulence. Figure 3 shows the (k_x, k_y) -section of the time-averaged 3D spectra of all four Elsässer fields \bar{Z}_p^\pm and \bar{Z}_s^\pm in Fourier space at a given $k_z = 2$ where they reach high values. These spectra appear similar because the turbulence is on average balanced and exhibit pronounced anisotropy due to shear with more power being in the $k_x k_y > 0$ region than in $k_x k_y < 0$, as also observed in other studies of shear MHD turbulence [33, 41–43, 58]. This type of anisotropy arises because Alfvén wave modes undergo linear non-modal growth as their time-varying k_x drifts in Fourier space from the region $k_x k_y < 0$ to $k_x k_y > 0$ [41, 45]. Arising from the shear, this spectral anisotropy is topologically distinct from that caused by a background field in forced shearless MHD turbulence (e.g., [4–6]).

Figure 4 shows the 1D spectra of the Elsässer fields in the perpendicular (k_x and k_z) and parallel (k_y) directions

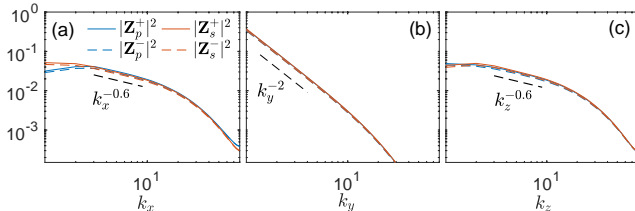


FIG. 4. 1D spectra of $|\bar{\mathbf{Z}}_p^\pm|^2$ and $|\bar{\mathbf{Z}}_s^\pm|^2$ represented as a function of (a) k_x , (b) k_y and (c) k_z being integrated in each case over the other two wavenumbers.

to the base flow and background field, which are obtained by integrating their 3D spectra over the other two directions. These 1D spectra also appear to be identical for each PAWs and SAWs, implying that balance occurs in fact over a broad range of scales. They differ most notably along k_x and k_y , with the latter being steeper than the former, which is a consequence of the anisotropy of the 3D spectra in the (k_x, k_y) -plane (Fig. 4). On the other hand, the 1D spectra along k_x and k_z are mostly similar with only a slight difference at low wavenumbers. The k_y -spectra follow k_y^{-2} as it is in forced MHD turbulence [59]. However, the spectra along k_x and k_z , which follow the same power-laws $k_x^{-0.6}$ and $k_z^{-0.6}$ at intermediate wavenumbers, differ from the classical ones $k^{-5/3}$ or $k^{-3/2}$ [4, 8, 16, 60] due to the shear.

In this Letter, we studied the dynamics of MHD turbulence in shear flows with a uniform streamwise magnetic field in the super-Alfvénic regime, focusing on the effect of shear on its balanced/imbalanced nature. We demonstrated the reduction of the turbulence imbalance for any initial conditions with increasing Alfvén Mach

number M_A , indicating that for sufficiently strong shear – already for $M_A \approx 10$, i.e., in the strongly super-Alfvénic regime – the turbulence is definitely balanced. By contrast, in classical forced shearless MHD turbulence, the degree of imbalance is conserved. We showed that the dynamics of pseudo- and shear-Alfvén waves, which are the building blocks of MHD turbulence, is governed by shear-induced linear non-modal processes – transient growth (over-reflection) and mode coupling. The transient, or non-modal growth of these waves supplies energy to turbulence, whereas the linear coupling leads to energy exchange and equipartition between pseudo- and shear-Alfvén waves as well as between the counter-propagating components \mathbf{Z}^\pm each of this wave type, ultimately leading to a balanced state.

In conclusion, the balancing of MHD turbulence at sufficiently large shear revealed in this Letter is consistent with recent solar wind observations [30] and may provide interpretation of these observations within the framework of sheared MHD turbulence dynamics. Of course, in reality, many other factors (e.g., thermodynamic complexity) are involved in solar wind dynamics, which have not been considered here. However, as mentioned above, shear remains a primary driver of turbulence. Further studies will allow us to understand how thermodynamic effects, such as pressure anisotropy, influence the balance/imbalance properties of solar wind turbulence.

This work is supported by the Deutsche Forschungsgemeinschaft (DFG) (Grant No. MA10950/1-1) and Shota Rustaveli National Science Foundation of Georgia (SRNSFG) (Grant No. FR-23- 1277).

[1] P. S. Iroshnikov, Turbulence of a Conducting Fluid in a Strong Magnetic Field, Sov. Astron. **7**, 566 (1964).

[2] R. H. Kraichnan, Inertial-Range Spectrum of Hydromagnetic Turbulence, Phys. Fluids **8**, 1385 (1965).

[3] A. Kolmogorov, The Local Structure of Turbulence in Incompressible Viscous Fluid for Very Large Reynolds' Numbers, Akad. Nauk SSSR Doklady **30**, 301 (1941).

[4] P. Goldreich and S. Sridhar, Toward a Theory of Interstellar Turbulence. II. Strong Alfvénic Turbulence, Astrophys. J. **438**, 763 (1995).

[5] J. Cho and E. T. Vishniac, The anisotropy of magnetohydrodynamic alfvénic turbulence, Astrophys. J. **539**, 273 (2000).

[6] J. Maron and P. Goldreich, Simulations of Incompressible Magnetohydrodynamic Turbulence, Astrophys. J. **554**, 1175 (2001).

[7] Y. Lithwick and P. Goldreich, Imbalanced weak magnetohydrodynamic turbulence, Astrophys. J. **582**, 1220 (2003).

[8] Y. Lithwick, P. Goldreich, and S. Sridhar, Imbalanced strong MHD turbulence, Astrophys. J. **655**, 269 (2007).

[9] J. C. Perez and S. Boldyrev, Numerical Simulations of Imbalanced Strong Magnetohydrodynamic Turbulence, The Astrophys. J. Lett. **710**, L63 (2010).

[10] A. Beresnyak and A. Lazarian, Strong imbalanced turbulence, Astrophys. J. **682**, 1070 (2008).

[11] A. Beresnyak and A. Lazarian, Scaling Laws And Diffuse Locality Of Balanced And Imbalanced Magnetohydrodynamic Turbulence, Astrophys. J. Lett. **722**, L110 (2010).

[12] J. W. Belcher and L. Davis, Large-amplitude Alfvén waves in the interplanetary medium, 2, J. Geophys. Res. Atmosph. **76**, 3534 (1971).

[13] C. W. Smith, K. Hamilton, and B. J. Vasquez, Variance Anisotropy in the Inertial Range, in *Solar Wind 11/SOHO 16, Connecting Sun and Heliosphere*, ESA Special Publication, Vol. 592, edited by B. Fleck, T. H. Zurbuchen, and H. Lacoste (2005) p. 551.

[14] L.-L. Zhao, G. P. Zank, L. Adhikari, D. Telloni, M. Stevens, J. C. Kasper, S. D. Bale, and N. E. Raouafi, Turbulence and Waves in the Sub-Alfvénic Solar Wind Observed by the Parker Solar Probe during Encounter 10, Astrophys. J. Lett. **934**, L36 (2022).

[15] L. Yang, J. He, D. Verscharen, H. Li, T. A. Bowen, S. D. Bale, H. Wu, W. Li, Y. Wang, L. Zhang, X. Feng, and Z. Wu, Energy transfer of imbalanced alfvénic turbulence in the heliosphere, Nat. Commun. **14**, 7955 (2023).

[16] J. C. Perez, J. Mason, S. Boldyrev, and F. Cattaneo, On the Energy Spectrum of Strong Magnetohydrodynamic

Turbulence, Phys. Rev. X **2**, 041005 (2012).

[17] N. Yokoi, Transport in Helical Fluid Turbulence, in *Helicities in Geophysics, Astrophysics, and Beyond*, Vol. 283, edited by K. Kuzanyan, N. Yokoi, M. K. Georgoulis, and R. Stepanov (2024) pp. 25–50.

[18] B. Teaca, M. S. Weidl, F. Jenko, and R. Schlickeiser, Acceleration of particles in imbalanced magnetohydrodynamic turbulence, Phys. Rev. E **90** (2014).

[19] P. J. J. Coleman, Turbulence, viscosity, and dissipation in the Solar-Wind plasma, Astrophys. J. **153**, 371 (1968).

[20] D. A. Roberts, L. W. Klein, M. L. Goldstein, and W. H. Matthaeus, The nature and evolution of magnetohydrodynamic fluctuations in the solar wind: Voyager observations, J. Geophys. Res. **92**, 11021 (1987).

[21] D. A. Roberts, M. L. Goldstein, L. W. Klein, and W. H. Matthaeus, Origin and evolution of fluctuations in the solar wind: Helios observations and Helios-Voyager comparisons, J. Geophys. Res. **92**, 12023 (1987).

[22] D. A. Roberts, M. L. Goldstein, W. H. Matthaeus, and S. Ghosh, Velocity shear generation of solar wind turbulence, J. Geophys. Res. **97**, 17115 (1992).

[23] W. H. Matthaeus, J. Minnie, B. Breech, S. Parhi, J. W. Bieber, and S. Oughton, Transport of cross helicity and radial evolution of Alfvénicity in the solar wind, Geophys. Res. Lett. **31**, L12803 (2004).

[24] B. Breech, W. H. Matthaeus, J. Minnie, S. Oughton, S. Parhi, J. W. Bieber, and B. Bavassano, Radial evolution of cross helicity in high-latitude solar wind, Geophys. Res. Lett. **32** (2005).

[25] B. Bavassano, E. Pietropaolo, and R. Bruno, Cross-helicity and residual energy in solar wind turbulence: Radial evolution and latitudinal dependence in the region from 1 to 5 AU, J. Geophys. Res. **103** (1998).

[26] J. E. Borovsky, The plasma structure of coronal hole solar wind: Origins and evolution, J. Geophys. Res. Space Phys. **121**, 5055 (2016).

[27] J. E. Borovsky, M. H. Denton, and C. W. Smith, Some Properties of the Solar Wind Turbulence at 1 AU Statistically Examined in the Different Types of Solar Wind Plasma, J. Geophys. Res. Space Phys. **124**, 2406 (2019).

[28] M. Iovieno, L. Gallana, F. Fraternale, J. Richardson, M. Opher, and D. Tordella, Cross and magnetic helicity in the outer heliosphere from Voyager 2 observations, Eur. J. Mech. B/Fluids **55**, 394 (2015).

[29] T. N. Parashar, M. L. Goldstein, B. A. Maruca, W. H. Matthaeus, D. Ruffolo, R. Bandyopadhyay, R. Chhiber, A. Chasapis, R. Qudsi, D. Vech, D. A. Roberts, S. D. Bale, J. W. Bonnell, T. D. De Wit, K. Goetz, P. R. Harvey, R. J. MacDowall, D. Malaspina, M. Pulupa, J. C. Kasper, K. E. Korreck, A. W. Case, M. Stevens, P. Whittlesey, D. Larson, R. Livi, M. Velli, and N. Raouafi, Measures of scale-dependent alfvénicity in the first PSP solar encounter, Astrophys. J. Suppl. Ser. **246**, 58 (2020).

[30] J. E. Soljento, S. W. Good, A. Osmane, and E. K. J. Kilpua, Imbalanced turbulence modified by large-scale velocity shears in the solar wind, Astrophys. J. Lett. **946**, L19 (2023).

[31] J. C. Perez and S. Boldyrev, Strong magnetohydrodynamic turbulence with cross helicity, Phys. Plasmas **17**, 055903 (2010).

[32] W. Horton, J.-H. Kim, G. D. Chagelishvili, J. C. Bowman, and J. G. Lominadze, Angular redistribution of nonlinear perturbations: A universal feature of nonuniform flows, Phys. Rev. E **81**, 066304 (2010).

[33] G. R. Mamatsashvili, D. Z. Gogichaishvili, G. D. Chagelishvili, and W. Horton, Nonlinear transverse cascade and two-dimensional magnetohydrodynamic subcritical turbulence in plane shear flows, Phys. Rev. E **89**, 043101 (2014).

[34] G. Mamatsashvili, G. Khujadze, G. Chagelishvili, S. Dong, J. Jiménez, and H. Foysi, Dynamics of homogeneous shear turbulence: A key role of the nonlinear transverse cascade in the bypass concept, Phys. Rev. E **94**, 023111 (2016).

[35] P. J. Schmid and D. S. Henningson, *Stability and Transition in Shear Flows* (Berlin: Springer, 2001).

[36] P. J. Schmid, Nonmodal Stability Theory, Annu. Rev. Fluid Mech. **39**, 129 (2007).

[37] R. R. Kerswell, Nonlinear Nonmodal Stability Theory, Ann. Rev. Fluid Mech. **50**, 319 (2018).

[38] A. E. Fraser, A. K. Kaminski, and J. S. Oishi, Nonmodal growth and optimal perturbations in magnetohydrodynamic shear flows, arXiv e-prints , arXiv:2510.03141 (2025).

[39] G. Chagelishvili, J.-N. Hau, G. Khujadze, and M. Oberlack, Mechanical picture of the linear transient growth of vortical perturbations in incompressible smooth shear flows, Physical Review Fluids **1**, 043603 (2016).

[40] D. Gogichaishvili, G. Mamatsashvili, W. Horton, and G. Chagelishvili, Active Modes and Dynamical Balances in MRI Turbulence of Keplerian Disks with a Net Vertical Magnetic Field, Astrophys. J. **866**, 134 (2018).

[41] D. Gogichaishvili, G. Mamatsashvili, W. Horton, G. Chagelishvili, and G. Bodo, Nonlinear Transverse Cascade and Sustenance of MRI Turbulence in Keplerian Disks with an Azimuthal Magnetic Field, Astrophys. J. **845**, 70 (2017).

[42] G. Mamatsashvili, G. Chagelishvili, M. E. Pessah, F. Steffani, and G. Bodo, Zero Net Flux MRI Turbulence in Disks: Sustenance Scheme and Magnetic Prandtl Number Dependence, Astrophys. J. **904**, 47 (2020).

[43] L. E. Held and G. Mamatsashvili, MRI turbulence in accretion discs at large magnetic Prandtl numbers, Mon. Not. R. Astron. Soc. **517**, 2309 (2022).

[44] G. Gogoberidze, G. D. Chagelishvili, R. Z. Sagdeev, and D. G. Lominadze, Linear coupling and overreflection phenomena of magnetohydrodynamic waves in smooth shear flows, Phys. Plasmas **11**, 4672 (2004).

[45] D. Gogichaishvili, G. Chagelishvili, R. Chanishvili, J. Lominadze, and Lominadze, Nature and dynamics of overreflection of Alfvén waves in MHD shear flows, J. Plasma Phys. **80**, 667 (2014).

[46] S. Boldyrev and J. C. Perez, Spectrum of weak magnetohydrodynamic turbulence, Phys. Rev. Lett. **103** (2009).

[47] V. A. Romanov, Stability of plane-parallel Couette flow, Functional Analysis and Its Applications **7**, 137 (1973).

[48] M. E. Stern, Joint Instability of Hydromagnetic Fields which are Separately Stable, Phys. Fluids **6**, 636 (1963).

[49] G. I. Ogilvie and J. E. Pringle, The non-axisymmetric instability of a cylindrical shear flow containing an azimuthal magnetic field, Mon. Not. R. Astron. Soc. **279**, 152 (1996).

[50] H. K. Moffatt, *Magnetic field generation in electrically conducting fluids* (Cambridge Univ. Press, 1978).

[51] J. Mason, F. Cattaneo, and S. Boldyrev, Dynamic Alignment in Driven Magnetohydrodynamic Turbulence, Phys. Rev. Lett. **97**, 255002 (2006).

[52] G. Lesur and P.-Y. Longaretti, Impact of dimensionless

numbers on the efficiency of magnetorotational instability induced turbulent transport, *Mon. Not. R. Astron. Soc.* **378**, 1471 (2007).

[53] J. F. Hawley, C. F. Gammie, and S. A. Balbus, Local Three-dimensional Magnetohydrodynamic Simulations of Accretion Disks, *Astrophys. J.* **440**, 742 (1995).

[54] O. M. Umurhan and O. Regev, Hydrodynamic stability of rotationally supported flows: Linear and nonlinear 2D shearing box results, *Astron. Astrophys.* **427**, 855 (2004).

[55] G. Lesur and P.-Y. Longaretti, On the relevance of sub-critical hydrodynamic turbulence to accretion disk transport, *Astron. Astrophys.* **444**, 25 (2005).

[56] A. Pumir, Turbulence in homogeneous shear flows, *Phys. Fluids* **8**, 3112 (1996).

[57] L. K. Jian, C. T. Russell, and J. G. Luhmann, Comparing Solar Minimum 23/24 with Historical Solar Wind Records at 1 AU, *Sol. Phys.* **274**, 321 (2011).

[58] G. C. Murphy and M. E. Pessah, On the Anisotropic Nature of MRI-driven Turbulence in Astrophysical Disks, *Astrophys. J.* **802**, 139 (2015).

[59] A. Beresnyak, On the Parallel Spectrum in Magnetohydrodynamic Turbulence, *Astrophys. J. Lett.* **801**, L9 (2015).

[60] S. Boldyrev, Spectrum of Magnetohydrodynamic Turbulence, *Phys. Rev. Lett.* **96**, 115002 (2006).